

The submitted manuscript has been authored by a contractor of the U. S. Government under contract No. W-31-109-ENG-38. Accordingly, the U. S. Government retains a nonexclusive, royalty-free license to publish or reproduce the published form of this contribution, or allow others to do so, for U. S. Government purposes.

RECEIVED

JUL 18 1996

OSTI

ANL-HEP-CP-96-51

hep-ph/9606421

June 21, 1996

CONF-960581--1

CALCULATION OF THE CROSS SECTION FOR TOP QUARK PRODUCTION *

EDMOND L. BERGER

High Energy Physics Division, Argonne National Laboratory, Argonne, IL 60439-4815, USA

E-mail: ELB@hep.anl.gov

and

HARRY CONTOPANAGOS

High Energy Physics Division, Argonne National Laboratory, Argonne, IL 60439-4815, USA

E-mail: CONTOPAN@hep.anl.gov

ABSTRACT

We summarize calculations of the cross section for top quark production at hadron colliders within the context of perturbative quantum chromodynamics, including resummation of the effects of initial-state soft gluon radiation to all orders in the strong coupling strength. In our approach we resum the universal leading-logarithm contributions, and we restrict the calculation to the region of phase space that is demonstrably perturbative. We compare our approach with other methods. We present predictions of the physical cross section as a function of the top quark mass in proton-antiproton reactions at center-of-mass energies of 1.8 and 2.0 TeV, and we discuss estimated uncertainties.

1. Introduction and Motivation

In this report we summarize calculations carried out in perturbative quantum chromodynamics (QCD) of the inclusive cross section for the production of top quark-antiquark ($t\bar{t}$) pairs in hadron reactions^{1,2,3,4}. We begin with a discussion of the motivation for the inclusion of the effects of initial state soft gluon radiation to all orders in the QCD coupling strength, and we review the general formalism of resummation. We outline the method and domain of applicability of perturbative resummation that we developed in the past year^{2,3}, and we contrast this approach with other methods^{1,4}. We present predictions of the physical cross section as a function of the top quark mass in proton-antiproton reactions at center-of-mass energies of 1.8 and 2.0 TeV.

In hadron interactions at collider energies, $t\bar{t}$ pair production proceeds through partonic hard-scattering processes involving initial-state light quarks q and gluons

*Invited paper presented by E. L. Berger at the XIth Topical Workshop on Hadron Collider Physics, Abano Terme, Padova, Italy, May, 1996

DISCLAIMER

Portions of this document may be illegible in electronic image products. Images are produced from the best available original document.

g. In lowest-order QCD, $\mathcal{O}(\alpha_s^2)$, the two partonic subprocesses are $q + \bar{q} \rightarrow t + \bar{t}$ and $g + g \rightarrow t + \bar{t}$. Calculations of the cross section through next-to-leading order, $\mathcal{O}(\alpha_s^3)$, involve gluonic radiative corrections to these lowest-order subprocesses as well as contributions from the $q + g$ initial state⁵. A complete fixed-order calculation at order $\mathcal{O}(\alpha_s^n)$, $n \geq 4$ does not exist.

The physical cross section for each production channel is obtained through the factorization theorem,

$$\sigma_{ij}(S, m^2) = \frac{4m^2}{S} \int_0^{\frac{s}{4m^2}-1} d\eta \Phi_{ij} \left[\frac{4m^2}{S}(1 + \eta), \mu^2 \right] \hat{\sigma}_{ij}(\eta, m^2, \mu^2). \quad (1)$$

The square of the total hadronic center-of-mass energy is S , the square of the partonic center-of-mass energy is s , and m denotes the top mass. The variable $\eta = \frac{s}{4m^2} - 1$ measures the distance from the partonic threshold. The indices $ij \in \{q\bar{q}, gg\}$ denote the initial parton channel. The partonic cross section $\hat{\sigma}_{ij}(\eta, m^2, \mu^2)$ is obtained commonly from fixed-order QCD calculations⁵, or, as described here, from calculations that go beyond fixed-order perturbation theory through the inclusion of gluon resummation^{1,2,3,4}. The parton flux is $\Phi_{ij}(y, \mu^2) = \int_y^1 \frac{dx}{x} f_{i/h_1}(x, \mu^2) f_{j/h_2}(y/x, \mu^2)$, where $f_{i/h_1}(x, \mu^2)$ is the density of partons of type i in hadron h_1 . Henceforth, we use the notation $\alpha(\mu) \equiv \alpha_s(\mu)/\pi$, where μ is the common renormalization/factorization scale of the problem. Unless otherwise specified, $\alpha \equiv \alpha(\mu = m)$. The total physical cross section is obtained after incoherent addition of the contributions from the $q\bar{q}$ and gg production channels. We ignore the small contribution from the qg channel.

A comparison of the partonic cross section at next-to-leading order with its lowest-order value reveals that the ratio becomes very large in the near-threshold region, i.e., the “ K -factor” at the partonic level $\hat{K}(\eta)$ becomes very large as $\eta \rightarrow 0$. An illustration of this behavior may be seen in Fig. 7 of Ref. [3]. This large ratio casts doubt on the reliability of simple fixed-order perturbation theory for physical processes for which the near-threshold region in the subenergy variable contributes significantly to the physical cross section. Top quark production at the Fermilab Tevatron is one such process, because the top mass is relatively large compared to the energy available. Other examples include the production of hadronic jets that carry large values of transverse momentum and the production of pairs of supersymmetric particles with large mass. To obtain more reliable theoretical estimates of the cross section in perturbative QCD, it is important first to identify and isolate the terms that provide the large next-to-leading order enhancement and then to resum these effects to all orders in the strong coupling strength.

2. Gluon Radiation and Resummation

The origin of the large threshold enhancement may be traced to initial-state gluonic radiative corrections to the lowest-order channels. Consider the subprocess

$i(k_1) + j(k_2) \rightarrow t(p_1) + \bar{t}(p_2) + g(k)$. We define the variable z through the partonic invariants¹

$$s = (k_1 + k_2)^2, \quad t_1 = (k_2 - p_2)^2 - m^2, \quad u_1 = (k_1 - p_2)^2 - m^2, \quad (1-z)m^2 = s + t_1 + u_1. \quad (2)$$

Alternatively, $(1-z) = \frac{2k \cdot p_1}{m^2}$. In the limit that $z \rightarrow 1$, the radiated gluon carries zero momentum. After cancellation of soft singularities and factorization of collinear singularities in $\mathcal{O}(\alpha^3)$, there are left-over integrable logarithmic contributions to the cross section associated with initial-state gluon radiation. These contributions are proportional to $\ln(1-z)$.

The partonic cross section may be expressed generally as

$$\hat{\sigma}_{ij}(\eta, m^2) = \int_{z_{min}}^1 dz \left[1 + \mathcal{H}_{ij}(z, \alpha) \right] \hat{\sigma}'_{ij}(\eta, m^2, z). \quad (3)$$

We work in the $\overline{\text{MS}}$ factorization scheme in which the q , \bar{q} and g densities and the next-to-leading order partonic cross sections are defined unambiguously. The lower limit of integration, $z_{min} = 1 - 4(1+\eta) + 4\sqrt{1+\eta}$, is set by kinematics. The derivative $\hat{\sigma}'_{ij}(\eta, m^2, z) = d(\hat{\sigma}_{ij}^{(0)}(\eta, m^2, z))/dz$, and $\hat{\sigma}_{ij}^{(0)}$ is the lowest-order $\mathcal{O}(\alpha^2)$ partonic cross section expressed in terms of inelastic kinematic variables to account for the emitted radiation.

Keeping only the leading logarithmic contributions through $\mathcal{O}(\alpha^3)$, we may write the total partonic cross section as

$$\hat{\sigma}_{ij}^{(0+1)}(\eta, m^2) = \int_{z_{min}}^1 dz \left\{ 1 + \alpha 2C_{ij} \ln^2(1-z) \right\} \hat{\sigma}'_{ij}(\eta, z, m^2), \quad (4)$$

where $C_{q\bar{q}} = C_F = 4/3$ and $C_{gg} = C_A = 3$. As is illustrated in Fig. 1(a), the leading logarithmic contribution, integrated over the near-threshold region $1 \geq z \geq 0$, provides an excellent approximation to the exact full next-to-leading order physical cross section as a function of the top quark mass. Although an exact fixed-order $\mathcal{O}(\alpha^4)$ calculation of $t\bar{t}$ pair production does not exist, we may invoke universality with massive lepton-pair production ($l\bar{l}$), the Drell-Yan process, to generalize Eq. (4) to higher order. In the near-threshold region, the kernel becomes

$$\mathcal{H}_{ij}^{(0+1+2)}(z, \alpha) \simeq 2\alpha C_{ij} \ln^2(1-z) + \alpha^2 \left[2C_{ij}^2 \ln^4(1-z) - \frac{4}{3} C_{ij} b_2 \ln^3(1-z) \right]. \quad (5)$$

The coefficient $b_2 = (11C_A - 2n_f)/12$, and the number of flavors $n_f = 5$. The further enhancement of the physical cross section produced by the $\mathcal{O}(\alpha^4)$ leading logarithmic terms in the near-threshold region is shown in Fig. 1. At $m = 175$ GeV, we compute the following ratios of the physical cross sections in the leading logarithmic approximation: $\sigma_{ij}^{(0+1)}/\sigma_{ij}^{(0)} = 1.22$, and $\sigma_{ij}^{(0+1+2)}/\sigma_{ij}^{(0+1)} = 1.14$. These ratios show that the near-threshold logarithms build up cross section in a worrisome

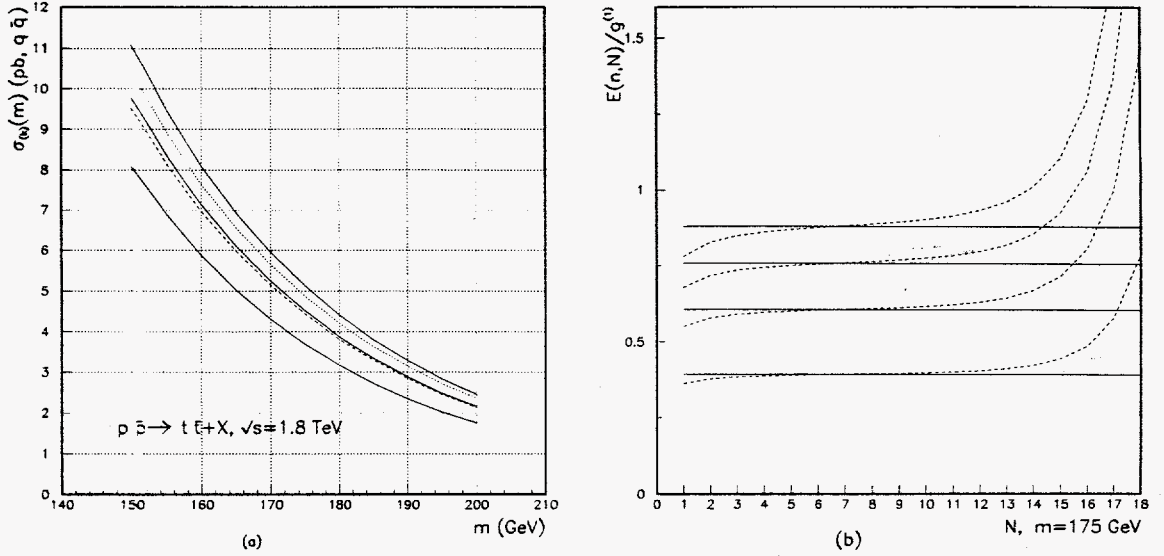


Fig. 1. (a) Physical cross sections in the $q\bar{q}$ channel in the $\overline{\text{MS}}$ scheme. The solid lines denote the finite-order partial sums of the universal leading-logarithmic contributions from the explicit $\mathcal{O}(\alpha^3)$ and $\mathcal{O}(\alpha^4)$ calculations for the $t\bar{t}$ and Drell-Yan cross sections, respectively. Lower solid: $\sigma^{(0)}$; middle solid: $\sigma^{(0+1)}$; upper solid: $\sigma^{(0+1+2)}$. The dashed curve represents the exact next-to-leading order calculation for $t\bar{t}$ production, in excellent agreement with $\sigma^{(0+1)}$. The dotted curve is our resummed prediction. (b) Optimum number of perturbative terms in the exponent with PVR (solid family is for PVR, dashed for perturbative approximation, both families increasing, for parametric values $n = 10, 20, 30, 40$).

fashion. The ratios suggest that perturbation theory is not converging to a stable prediction of the cross section.

The goal of gluon resummation is to sum the series in $\alpha^n \ln^{2n}(1-z)$ to all orders in α in order to obtain a more defensible prediction. This procedure has been studied extensively for the Drell-Yan process⁶. In essentially all resummation procedures, the large logarithmic contributions are exponentiated into a function of the QCD running coupling strength, itself evaluated at a variable momentum scale that is a measure of the radiated gluon momentum. For example, in the approach of LSvN¹, the resummed partonic cross section is written as

$$\hat{\sigma}_{ij}^{R,IRC}(\eta, \mu_o) = \int_{z_{\min}}^{1-(\mu_o/m)^3} dz e^{E_{ij}(z, m^2)} \hat{\sigma}'_{ij}(\eta, m^2, z), \quad (6)$$

where the exponent

$$E_{ij}(z, m^2) \propto C_{ij} \alpha ((1-z)^{2/3} m^2) \ell n^2(1-z). \quad (7)$$

Different methods of resummation differ in theoretically and phenomenologically important respects. Formally, if not explicitly in some approaches, an integral over the radiated gluon momentum z must be done over regions in which $z \rightarrow 0$. Therefore, one significant distinction among methods has to do with how the inevitable “non-perturbative” region is handled in each case. Examination of Eqs. (6) and (7) shows

that an infrared singularity is encountered in the soft-gluon limit $z \rightarrow 1$: owing to the logarithmic behavior of $\alpha(q^2)$, $\alpha(q^2) \propto \ln^{-1}(q^2/\Lambda_{QCD}^2)$, $\alpha((1-z)^{2/3}m^2) \rightarrow \infty$ as $z \rightarrow 1$. The infrared singularity is a manifestation of non-perturbative physics. In the approach of LSvN, this divergence of the integrand at the upper limit of integration necessitates introduction of the undetermined infrared cutoff (IRC) μ_o in Eq. (6), with $\Lambda_{QCD} \leq \mu_o \leq m$. The cutoff prevents the integration over z from reaching the Landau pole of the QCD running coupling constant. The presence of an extra scale spoils the renormalization group properties of the overall expression. The unfortunate dependence of the resummed cross section on this undetermined cutoff is important numerically since it appears in an exponent¹. It is difficult to evaluate theoretical uncertainties in a method that depends on an undetermined infrared cutoff.

3. Perturbative Resummation

The method of resummation we employ^{2,3} is based on a perturbative truncation of principal-value resummation. The principal-value method (PVR)⁶ has an important technical advantage in that it does not depend on arbitrary infrared cutoffs, as all Landau-pole singularities are by-passed by a Cauchy principal-value prescription. Because extra undetermined scales are absent, the method also permits an evaluation of the perturbative regime of applicability of the method, i.e., the region of the gluon radiation phase space where perturbation theory should be valid.

To illustrate how infrared cutoffs are avoided in the PVR method, it is useful to begin with an expression in moment (n) space for the exponent that resums the $\ln(1-z)$ terms⁷. Factorization and evolution lead directly to exponentiation in moment space:

$$E(n, m^2) = - \int_0^1 dx \frac{x^{n-1} - 1}{1-x} \int_{(1-x)^2}^1 \frac{d\lambda}{\lambda} g[\alpha(\lambda m^2)]. \quad (8)$$

The function $g(\alpha)$ is calculable perturbatively, but the behavior of $\alpha(\lambda m^2)$ leads to a divergence of the integrand when $\lambda m^2 \rightarrow \Lambda_{QCD}^2$. To tame the divergence, a cutoff can be introduced in the integral over x or directly in momentum space, in the fashion of LSvN. In the principal-value redefinition of resummation, the singularity is avoided by replacement of the integral over the real axis x in Eq. (8) by an integral in the complex plane along a contour P that is symmetric under reflections across the real axis:

$$E^{PV}(n, m^2) \equiv - \int_P d\zeta \frac{\zeta^{n-1} - 1}{1-\zeta} \int_{(1-\zeta)^2}^1 \frac{d\lambda}{\lambda} g[\alpha(\lambda m^2)]. \quad (9)$$

The function $E^{PV}(n, m^2)$ is finite since the Landau pole singularity is by-passed. In Eq. (9), all large soft-gluon threshold contributions are included through the two-loop running of α .

Equations (8) and (9) have identical perturbative content, but they have different non-perturbative content since the infrared region is treated differently in the two cases. The non-perturbative content is not a prediction of perturbative QCD. In our study of top quark production, we choose to use the exponent only in the region of phase space in which the perturbative content dominates.

We use the attractive finiteness of Eq. (9) to derive a perturbative asymptotic representation of $E(x, \alpha(m))$ that is valid in the moment-space interval

$$1 < x \equiv \ln n < t \equiv \frac{1}{2\alpha b_2}. \quad (10)$$

This perturbative asymptotic representation is

$$E_{ij}(x, \alpha) \simeq E_{ij}(x, \alpha, N(t)) = 2C_{ij} \sum_{\rho=1}^{N(t)+1} \alpha^\rho \sum_{j=0}^{\rho+1} s_{j,\rho} x^j. \quad (11)$$

Here

$$s_{j,\rho} = -b_2^{\rho-1} (-1)^{\rho+j} 2^\rho c_{\rho+1-j} (\rho-1)! / j!, \quad (12)$$

and $\Gamma(1+z) = \sum_{k=0}^{\infty} c_k z^k$, where Γ is the Euler gamma function. The number of perturbative terms $N(t)$ in Eq. (11) is obtained³ by optimizing the asymptotic approximation $|E(x, \alpha) - E(x, \alpha, N(t))| = \text{minimum}$. Because of the range of validity in Eq. (10), terms in the exponent of the form $\alpha^k \ln^k n$ are of order unity, and terms with fewer powers of logarithms, $\alpha^k \ln^{k-m} n$, are negligible. This explains why resummation is completed in a finite number of steps. In addition, we discard monomials $\alpha^k \ln^k n$ in the exponent because of the restricted leading-logarithm universality between the $t\bar{t}$ and $l\bar{l}$ processes.

The exponent we use in our calculations of top quark production is the truncation

$$E_{ij}(x, \alpha, N) = 2C_{ij} \sum_{\rho=1}^{N(t)+1} \alpha^\rho s_\rho x^{\rho+1}, \quad (13)$$

with the coefficients $s_\rho \equiv s_{\rho+1,\rho} = b_2^{\rho-1} 2^\rho / \rho(\rho+1)$. The number of perturbative terms $N(t)$ is a function of only the top quark mass m . This expression contains no factorially-growing (renormalon) terms. The perturbative region of phase space is far removed from the part of phase space in which renormalons could be influential⁴.

In Fig. 1(b) we illustrate the validity of the asymptotic approximation for a value of t corresponding to $m = 175$ GeV. Optimization works perfectly, with $N(t) = 6$, and the plot demonstrates the typical breakdown of the asymptotic approximation if N were allowed to increase beyond $N(t)$. This is the exponential rise of the infrared (IR) renormalons, the $(\rho-1)!$ growth in the second term of Eq. (12). As long as n is in the interval of Eq. (10), all the members of the family in n are optimized at the

same $N(t)$, showing that the optimum number of perturbative terms is a function of t , i.e., of m only.

It is valuable to stress that we can derive the perturbative expressions, Eqs. (10), (11), and (12), from the unregulated exponent Eq. (8) without the PVR prescription, although with less certitude. We discuss this point in some detail in our long paper³.

After inversion of the Mellin transform from moment space to the physically relevant momentum space, the resummed partonic cross sections, including all large threshold corrections, can be written in the form of Eq. (3), but with Eq. (5) replaced by

$$\mathcal{H}_{ij}^R(z, \alpha) = \int_0^{\ln(\frac{1}{1-z})} dx e^{E_{ij}(x, \alpha)} \sum_{j=0}^{\infty} Q_j(x, \alpha). \quad (14)$$

The leading large threshold corrections are contained in the exponent $E_{ij}(x, \alpha)$, a calculable polynomial in x . The functions $\{Q_j(x, \alpha)\}$ arise from the analytical inversion of the Mellin transform from moment space to momentum space. These functions are produced by the resummation and are expressed in terms of successive derivatives of E : $P_k(x, \alpha) \equiv \partial^k E(x, \alpha)/k! \partial^k x$. Each Q_j contains j more powers of α than of x so that Eq. (14) embodies a natural power-counting of threshold logarithms.

The functional form of E_{ij} for $t\bar{t}$ production is identical to that for $l\bar{l}$ production, except for the identification of the two separate channels, denoted by the subscript ij . However, only the *leading* threshold corrections are universal. Final-state gluon radiation as well as initial-state/final-state interference effects produce sub-leading logarithmic contributions that differ for processes with different final states. Among all $\{Q_j\}$ in Eq. (14), only the very leading one is universal. This is the linear term in P_1 contained in Q_0 , that turns out to be P_1 itself. Since we intend to resum only the universal leading logarithms, we retain only P_1 . Hence, Eq. (14) can be integrated explicitly, and the resummed version of Eq. (3) is

$$\hat{\sigma}_{ij}^{R;pert}(\eta, m^2) = \int_{z_{min}}^{z_{max}} dz e^{E_{ij}(\ln(\frac{1}{1-z}), \alpha)} \hat{\sigma}'_{ij}(\eta, m^2, z). \quad (15)$$

The upper limit of integration in Eq. (15) is set by the boundary between the perturbative and non-perturbative regimes. An intuitive definition of the perturbative region, where inverse power terms are unimportant, is provided by the inequality $\frac{\Lambda_{QCD}}{(1-z)^m} \leq 1$. This inequality is identical to the expression in moment space, Eq. (10), with the identification $n = \ln \frac{1}{1-z}$. In momentum space, the same condition is realized by the constraint that all $\{Q_j\}$, $j \geq 1$ be small compared to Q_0 . From the explicit expressions³ for the $\{Q_j\}$, one may show that this constraint corresponds to

$$P_1 \left(\ln \left(\frac{1}{1-z} \right), \alpha \right) < 1. \quad (16)$$

Equation (16) is equivalent to the requirement that terms that are subleading according to perturbative power-counting are indeed subleading numerically; Eq. (16) is the essence of perturbation theory in this context.

As remarked above, we accept only the perturbative content of principal-value resummation, and our cross section is evaluated accordingly. Specifically, we use Eq. (15) with the upper limit of integration, z_{max} , calculated from Eq. (16). The upshot is an effective threshold cutoff on the integral over the scaled subenergy variable η , but one that is calculable, *not* arbitrary. Our perturbative resummation probes the threshold down to the point $\eta \geq \eta_0 = (1 - z_{max})/2$. Below this value, perturbation theory, resummed or otherwise, is not to be trusted. For the top mass $m = 175$ GeV, we determine that the perturbative regime is restricted to $\eta \geq 0.007$ for the $q\bar{q}$ channel and $\eta \geq 0.05$ for the gg channel. These numbers may be converted to more readily understood values of the subenergy above which we judge our perturbative approach is valid: at $m = 175$ GeV, these are 1.22 GeV above the threshold in the $q\bar{q}$ channel and 8.64 GeV above the threshold in the gg channel. The difference reflects the larger color factor in the gg case. A larger color factor makes the non-perturbative region larger. (One could attempt to apply Eq. (15) all the way to $z_{max} = 1$, i.e., to $\eta = 0$, but one would then be using a *model* for non-perturbative effects, the one suggested by PVR, below the region justified by perturbation theory.)

It is useful to comment on the differences between our approach to resummation and another method published recently by Catani *et al* (CMNT)⁴. We both use the same universal leading-logarithm expression in moment space, but differences occur after the transformation to momentum space. In this paper, we set aside comments on mathematical aspects of their procedure and focus instead on phenomenological issues of interest. As remarked above, the Mellin transformation generates subleading terms in momentum space. CMNT choose to retain all of these inasmuch as they perform the Mellin inversion numerically. Instead, in keeping with the fact that subleading logarithmic terms are not universal, we retain only the universal leading logarithm terms in momentum space, and we restrict our phase space integration to the region in which the subleading terms would not be numerically significant regardless. The differences in the two approaches can be stated more explicitly if we examine the perturbative expansion of the kernel $\mathcal{H}_{ij}^R(z, \alpha)$, Eq. (14). If, instead of restricting the resummation to the universal leading logarithms only, we were to use the full content of Eq. (14), we would arrive at an analytic expression that is equivalent to the numerical inversion of CMNT,

$$\mathcal{H}_{ij}^R \simeq 2\alpha C_{ij} \left[\ell n^2(1-z) - 2\gamma_E \ell n(1-z) \right] + \mathcal{O}(\alpha^2). \quad (17)$$

In terms of this expansion, in our work we retain only the leading term $\ell n^2(1-z)$ at order α , but CMNT retain both this term and the subleading term $-2\gamma_E \ell n(1-z)$. We judge that it is not justified to keep the subleading term for three reasons: it is not universal; it is not the same as the subleading term in the exact $\mathcal{O}(\alpha^3)$ calculation; and it can be changed arbitrarily if one elects to keep non-leading terms in moment space. As a practical matter, the subleading term is negative and numerically significant. In the $q\bar{q}$ channel at $m = 175$ GeV and $\sqrt{S} = 1.8$ TeV, its inclusion eliminates more

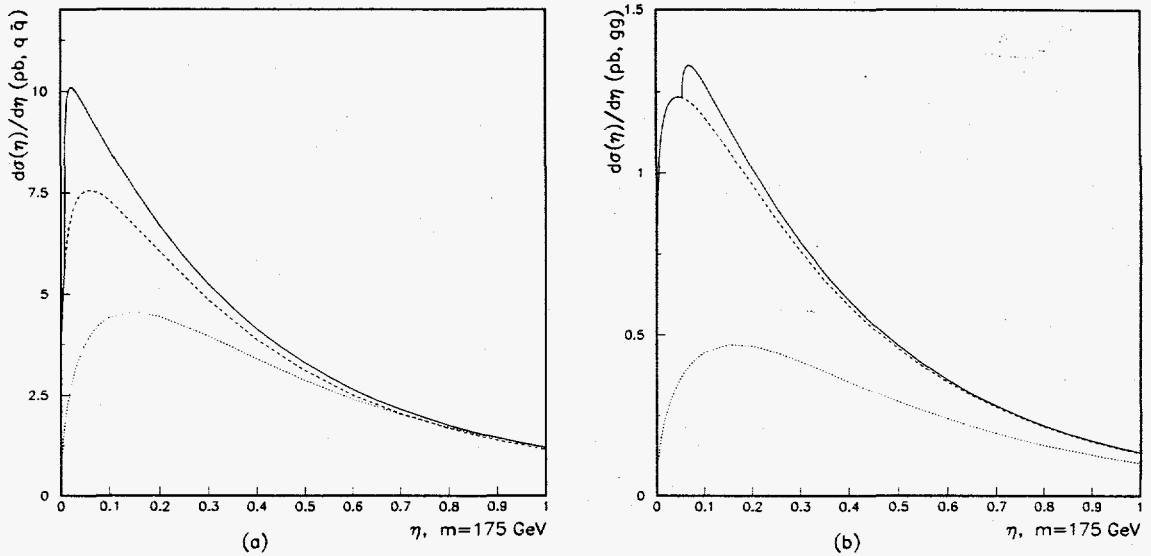


Fig. 2. Differential cross section $d\sigma/d\eta$ in the $\overline{\text{MS}}$ -scheme for the (a) $q\bar{q}$ and (b) gg channels: Born (dotted), NLO (dashed) and resummed (solid).

than half of the contribution from the leading term. In our view, the presence of numerically significant subleading contributions means that non-universal structures are not under control and begs the question of consistency⁸. A further justification for the retention of only the leading term is that it approximates the exact next-to-leading order result well, as shown in Fig. 1(a). The choice made by CMNT reproduces only one-third of the exact next-to-leading order result. The influence of subleading terms is amplified at higher orders where additional subleading structures occur in the CMNT approach with significant numerical coefficients proportional to π^2 , $\zeta(3)$, and so forth. Further comments about the different results in the two approaches are reserved to our discussion of predictions for cross sections at $\sqrt{S} = 1.8$ TeV.

4. Physical cross section

In order to achieve the best accuracy available we wish to include in our predictions as much as is known theoretically. Our final resummed partonic cross section can therefore be written^{2,3}

$$\hat{\sigma}_{ij}^{\text{pert}}(\eta, m^2, \mu^2) = \hat{\sigma}_{ij}^{\text{R,pert}}(\eta, m^2, \mu^2) - \hat{\sigma}_{ij}^{(0+1)}(\eta, m^2, \mu^2) \Big|_{\text{R,pert}} + \hat{\sigma}_{ij}^{(0+1)}(\eta, m^2, \mu^2). \quad (18)$$

The second term is the part of the partonic cross section up to one-loop that is included in the resummation, while the last term is the exact one-loop cross section⁵. To obtain physical cross sections, we insert Eq. (18) into Eq. (1), and we integrate over η . Other than the top mass, the only undetermined scales are the QCD factorization and renormalization scales. We adopt a common value μ for both, and we vary this

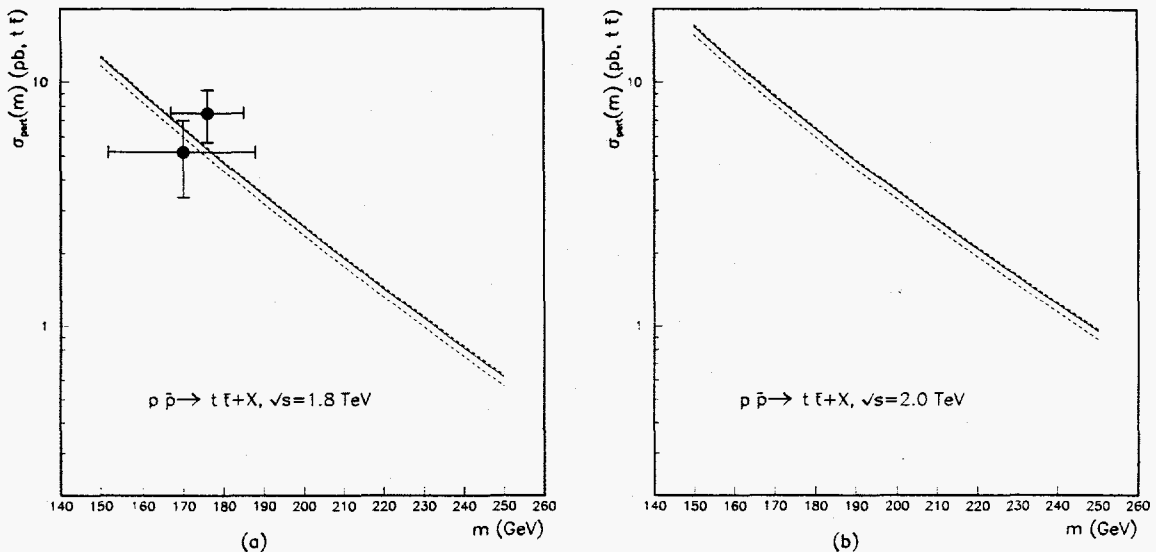


Fig. 3. Inclusive cross section for top quark production in the $\overline{\text{MS}}$ -scheme. The dashed curves show our perturbative uncertainty band, while the solid curve is our central prediction: (a) $\sqrt{S} = 1.8$ TeV and (b) $\sqrt{S} = 2$ TeV.

scale over the interval $\mu/m \in \{0.5, 2\}$ in order to evaluate the theoretical uncertainty of the numerical predictions. We use the CTEQ3M parton densities⁹.

A quantity of phenomenological interest is the differential cross section $\frac{d\sigma_{ij}(S, m^2, \eta)}{d\eta}$. Its integral over η is the total cross section. In Fig. 2 we plot these distributions for $m = 175$ GeV, $\sqrt{S} = 1.8$ TeV, and $\mu = m$. The full range of η extends to 25, but we display the behavior only in the near-threshold region where resummation is important. We observe that, at the energy of the Tevatron, resummation is significant for the $q\bar{q}$ channel and less so for the gg channel. In Fig. 1(a), the dotted curve shows that our final resummed cross section in the $q\bar{q}$ channel, after integration over all η , lies about half-way between the cross sections obtained from the near-threshold leading logarithms at orders $\mathcal{O}(\alpha^3)$ and $\mathcal{O}(\alpha^4)$.

We show our total $t\bar{t}$ -production cross section as a function of top mass in Fig. 3. The central value of our predictions is obtained with the choice $\mu/m = 1$, and the lower and upper limits are the maximum and minimum of the cross section in the range of the hard scale $\mu/m \in \{0.5, 2\}$. At $m = 175$ GeV, the full width of the uncertainty band is about 10%. We consider that the variation of the cross section over the range $\mu/m \in \{0.5, 2\}$ provides a good overall estimate of uncertainty. For comparison, we note that over the same range of μ , the strong coupling strength α varies by $\pm 10\%$ at $m = 175$ GeV. Our prediction of Fig. 3(a) is in agreement with the data¹⁰. We find $\sigma^{t\bar{t}}(m = 175 \text{ GeV}, \sqrt{S} = 1.8 \text{ TeV}) = 5.52^{+0.07}_{-0.42} \text{ pb}$. Our cross section is larger than the next-to-leading order value by about 9%. Using a different choice of parton densities¹¹, we find a 4% difference in the central value of our prediction² at $m = 175$ GeV. A comparison of the predictions³ in the $\overline{\text{MS}}$ and DIS factorization

schemes also shows a modest difference at the level of 4%.

In Fig. 3(b) we present our predictions for an upgraded Tevatron operating at $\sqrt{S} = 2$ TeV. We predict $\sigma^{t\bar{t}}(m = 175 \text{ GeV}, \sqrt{S} = 2 \text{ TeV}) = 7.56_{-0.55}^{+0.10} \text{ pb}$. The 2 pb increase in the predicted top quark cross section over its value at $\sqrt{S} = 1.8$ TeV is about a 37% gain.

Two other groups have published predictions for the cross section. At $m = 175$ GeV and $\sqrt{s} = 1.8$ TeV, the three values are: $\sigma^{t\bar{t}}(\text{BC}^{2,3}) = 5.52_{-0.42}^{+0.07} \text{ pb}$; $\sigma^{t\bar{t}}(\text{LSvN}^1) = 4.95_{-0.40}^{+0.70} \text{ pb}$; and $\sigma^{t\bar{t}}(\text{CMNT}^4) = 4.75_{-0.68}^{+0.63} \text{ pb}$. From the purely numerical point of view, all three predictions agree within their estimates of theoretical uncertainty. However, the resummation methods differ, as discussed above, the methods for estimating the uncertainties differ, and different parton sets are used. Comparing with LSvN¹, we find that our central values are 10 – 14% larger, and our estimated theoretical uncertainty is 9 – 10% compared with their 28% – 20%. Our Born cross section, however, is about 3 – 5% larger than the LSvN Born cross section due to the different parton distributions used in the two calculations. Both the central value and the band of uncertainty of the LSvN predictions are sensitive to their undetermined infrared cutoffs. To estimate theoretical uncertainty, we use the standard μ -variation, whereas LSvN obtain their uncertainty primarily from variations of their cutoffs. CMNT calculate a central value of the resummed cross section (also with $\mu/m = 1$) that is less than 1% above the exact next-to-leading order value. As explained earlier, the suppression of the effects of resummation arises from the retention by CMNT of numerically significant non-universal subleading logarithmic terms. Indeed, if the subleading term $-2\gamma_E \ln(1-z)$ is discarded in Eq. (17), the residuals $\delta_{ij}/\sigma_{ij}^{NLO}$ defined by CMNT⁴ increase from 0.18% to 1.3% in the $q\bar{q}$ production channel and from 5.4% to 20.2% in the gg channel¹². After addition of the two channels, the total residual δ/σ^{NLO} grows from the negligible value of about 0.8% cited by CMNT to the value 3.5%. While still smaller than the increase of about 9% that we obtain, the increase of 3.5% vs. 0.8% shows the substantial influence of the subleading logarithmic terms retained by CMNT. We explain above the reasons that we judge that our method is preferable theoretically.

Turning to pp scattering at the energies of the Large Hadron Collider (LHC) at CERN, we note a few significant differences from $p\bar{p}$ scattering at the energy of the Tevatron. The dominance of the $q\bar{q}$ production channel is replaced by gg dominance at the LHC. Owing to the much larger value of \sqrt{S} , the near-threshold region in the subenergy variable is relatively less important, reducing the significance of initial-state soft gluon radiation. Lastly, physics in the region of large subenergy, where straightforward next-to-leading order QCD is also inadequate, becomes significant for $t\bar{t}$ production at LHC energies. Using the approach described in this paper, we estimate $\sigma^{t\bar{t}}(m = 175 \text{ GeV}, \sqrt{S} = 14 \text{ TeV}) = 760 \text{ pb}$.

5. Discussion and Conclusions

In this paper, we summarize the calculation of the inclusive cross section for top quark production in perturbative QCD, including the resummation of initial-state gluon radiation to all orders. The advantages of the perturbative resummation method^{2,3} are that there are no arbitrary infrared cutoffs, and there is a well-defined perturbative region of applicability where subleading logarithmic terms are numerically suppressed. Our theoretical analysis shows that perturbative resummation without a model for non-perturbative behavior is both possible and advantageous. In perturbative resummation, the perturbative region of phase space is separated cleanly from the region of non-perturbative behavior. The former is the region where large threshold corrections exponentiate but behave in a way that is *perturbatively stable*. The asymptotic character of the QCD perturbative series, including large multiplicative color factors, is flat, and excursions around the optimum number of perturbative terms does not create numerical instabilities or intolerable scale-dependence. Infrared renormalons are far away from the stability plateau and, even though their presence is essential for defining this plateau, they are of no numerical consequence in the perturbative regime. Large color factors, which are multiplicative in the exponent, enhance the infrared renormalon effects and contribute significantly to limiting the perturbative regime.

Our resummed cross sections are about 9% above the next-to-leading order cross sections computed with the same parton distributions. The scale dependence of our cross section is fairly flat, resulting in a 9–10% theoretical uncertainty. This variation is smaller than the corresponding dependence of the next-to-leading cross section, as should be expected. In recent papers⁴, the authors state that the increase in cross section they find with their resummation method is of the order of 1% over next-to-leading order. The numerical difference in the two approaches boils down to the treatment of the subleading logarithms, which can easily shift the results by a few percent, if proper care is not taken. Our approach includes the universal leading logarithms only while theirs includes non-universal subleading structures which produce the suppression they find. In our opinion, their treatment of the subleading structures is not correct. The issue is one to be decided by the theory community; it is not one for experimental resolution.

Our theoretical analysis and the stability of our cross sections under μ variation provide confidence that our perturbative resummation procedure yields an accurate calculation of the inclusive top quark cross section at Tevatron energies and exhausts present understanding of the perturbative content of the theory. Our prediction agrees with data, within the large experimental uncertainties.

Extending our calculation to much larger values of m than shown in Fig. 3, we

find that resummation in the principal $q\bar{q}$ channel produces enhancements over the next-to-leading order cross section of 21%, 26%, and 34%, respectively, at $m = 500$, 600, and 700 GeV. The reason for the increase of the enhancements with mass at fixed energy is that the threshold region becomes increasingly dominant. Since the $q\bar{q}$ channel also dominates in the production of hadronic jets at very large values of transverse momenta, we suggest that on the order of 25% of the excess cross section reported by the CDF collaboration¹³ may well be accounted for by resummation.

This work was supported by the U.S. Department of Energy, Division of High Energy Physics, Contract No. W-31-109-ENG-38.

6. References

1. E. Laenen, J. Smith and W.L. van Neerven, Nucl. Phys. B369 (1992) 543; Phys. Lett. B321 (1994) 254.
2. E. L. Berger and H. Contopanagos, Phys. Lett. B361 (1995) 115 and Erratum.
3. E. L. Berger and H. Contopanagos, ANL-HEP-PR-95-82, hep-ph/9603326 (15 Mar 1996), Phys. Rev. D (in press).
4. S. Catani, M. Mangano, P. Nason and L. Trentadue, hep-ph/9602208 (1 Feb 1996); hep-ph/9604351 (18 Apr 1996).
5. P. Nason, S. Dawson and R.K. Ellis, Nucl. Phys. B303 (1988) 607; B327 (1989) 49; B335 (1990) 260 (E). W. Beenakker, H. Kuijif, W.L. van Neerven and J. Smith, Phys. Rev. D40 (1989) 54; W. Beenakker, W.L. van Neerven, R. Meng, G.A. Schuler and J. Smith, Nucl. Phys. B351 (1991) 507.
6. H. Contopanagos and G. Sterman, Nucl. Phys. B400 (1993) 211; B419 (1994) 77. L. Alvero and H. Contopanagos, Nucl. Phys. B436 (1995) 184; B456 (1995) 497.
7. G. Sterman, Nucl. Phys. B281 (1987) 310; S. Catani and L. Trentadue, Nucl. Phys. B327 (1989) 323; B353 (1991) 183; H. Contopanagos, E. Laenen and G. Sterman, hep-ph/9604313 (13 Apr 1996)
8. It is difficult professionally to critique in Italy the work of four esteemed Italian theorists, and it is uncomfortable personally as well. Stefano, Michelangelo, Paolo, and Luca are friends of many years. They believe they are correct, and we are confident that we are. Time will tell.
9. H.L. Lai et al., Phys. Rev. D51 (1995) 4763.
10. P. Azzi (CDF collaboration); P. Bhat (D0 collaboration), Proceedings of the XXXI Rencontres de Moriond, "QCD and High Energy Hadronic Interactions", March, 1996.
11. A. Martin, R. Roberts and W. J. Stirling, Phys. Lett. B354 (1995) 155.
12. We thank Michelangelo Mangano and Paolo Nason for supplying the residuals for their gg channel that are not included in Ref. [4].
13. F. Abe et al. (CDF Collaboration), FERMILAB-PUB-96/020-E, hep-ex/9601008 (19 Jan 1996), submitted to Phys. Rev. Lett.

DISCLAIMER

This report was prepared as an account of work sponsored by an agency of the United States Government. Neither the United States Government nor any agency thereof, nor any of their employees, makes any warranty, express or implied, or assumes any legal liability or responsibility for the accuracy, completeness, or usefulness of any information, apparatus, product, or process disclosed, or represents that its use would not infringe privately owned rights. Reference herein to any specific commercial product, process, or service by trade name, trademark, manufacturer, or otherwise does not necessarily constitute or imply its endorsement, recommendation, or favoring by the United States Government or any agency thereof. The views and opinions of authors expressed herein do not necessarily state or reflect those of the United States Government or any agency thereof.